



Published in final edited form as:

J Dent Res. 2010 July ; 89(7): 722–727. doi:10.1177/0022034510364492.

Human Temporomandibular Joint Eminence Shape and Load Minimization

L.R. Iwasaki^{1,*}, M.J. Crosby², D.B. Marx³, Y. Gonzalez⁴, W.D. McCall Jr.⁴, R. Ohrbach⁴, and J.C. Nickel¹

¹University of Missouri-Kansas City, School of Dentistry, Departments of Orthodontics & Dentofacial Orthopedics and Oral Biology, 650 E. 25th St., Kansas City, MO 64108-2784, USA

²Private Practice, Suwanee, GA 30024-8561, USA

³University of Nebraska, Department of Statistics, 340 Hardin Hall North, Lincoln, NE 68583-0963, USA

⁴University at Buffalo, School of Dental Medicine, Department of Oral Diagnostic Sciences, 355 Squire Hall, Buffalo, NY 14214, USA

Abstract

Analysis of previous data suggested the hypothesis that temporomandibular joint (TMJ) eminence shapes develop ideally to minimize joint loads. Hence, we tested this hypothesis in nine females and eight males in each of two groups, with and without TMJ disc displacement. Participants provided anatomical data used in a joint load minimization numerical model to predict, and jaw-tracking data used to measure, eminence shapes. Coordinate data (x,y) of shapes were fit to third-order polynomials for two sessions, sides, and methods (predicted, measured) for each participant. Inter-session data were reliable and averaged. Those with, compared with those without, disc displacement had higher measured shape range (5:1) and left-right asymmetry prevalence (4:1). In 29 symmetrical individuals, ANCOVA and Bonferroni tests compared vertical dimensions (y) at 11 postero-anterior points (x), 0.5 mm apart. Model-predicted and measured shapes were significantly different ($P \leq 0.01$) near the eminence crest, but joint load minimization was consistent with eminence shape for $x < 3.0$ mm.

Keywords

TMJ; human; numerical modeling; jaw tracking

Introduction

Relationships among neuromuscular control of temporomandibular joint (TMJ) loads, direction of joint loads as dictated by dental eruption, and growth of the TMJ eminence (Nickel *et al.*, 1988) suggest that the latter is consistent with a neuromuscular objective of joint load minimization. This hypothesis has been tested in a numerical model based on joint load minimization to predict effective sagittal TMJ eminence shapes in healthy humans (Iwasaki *et al.*, 2003a,b, 2004; Nickel *et al.*, 2002, 2003; Nickel and Iwasaki, 2004). Effective sagittal eminence shape is defined as the sagittal plane trajectory of the TMJ stress-field (Gallo *et al.*, 2000, 2006) during symmetrical mandibular protrusion and

*corresponding author, iwasakil@umkc.edu.

A supplemental appendix to this article is published electronically only at <http://jdr.sagepub.com/supplemental>.

retrusion. That is, on each side, this shape is given by the lateral view path of the minimum contact area between TMJ structures as condyles move symmetrically from positions when teeth are in maximum intercuspation to protrusion. This path is determined by soft- and hard-tissue shapes combined and delineates the so-called effective eminence. Subject-specific effective sagittal eminence shapes predicted by the model have shown acceptable accuracy (average errors $\leq 9\%$) when compared with measured shapes from the same individuals (Iwasaki *et al.*, 2003a,b; Nickel *et al.*, 2002, 2003; Nickel and Iwasaki, 2004).

Analysis of these data suggests that, in healthy humans, effective eminences have developed into shapes associated with low TMJ loads. This association could help maintain the mechanical integrity of joint tissues, because loads of high magnitude could cause fatigue-failure. Thus, if effective eminence shapes in a given individual were inconsistent with joint load minimization, TMJ forces during jaw loading conditions such as biting might be relatively high, and the individual may be at risk for degenerative TMJ changes.

Temporomandibular disorders (TMDs) are second only to low back pain among disabling musculoskeletal conditions and are at least twice as prevalent in women compared with men (NIDCR Web site, 2009). TMDs that involve disc displacement affect $> 25\%$ of the community and about 75% of clinical cases (LeResche, 1995). Human TMJ surfaces are highly incongruent, and the disc is the main source of lubrication and stress-distribution (Nickel *et al.*, 2001; Detamore and Athanasiou, 2003). Hence, any compromise to the disc may predispose the individual for degenerative TMJ changes, which, on average, tend to occur 15 yrs earlier than in post-cranial joints (*e.g.*, knee, hip), where loading surfaces are more congruent (Lawrence *et al.*, 1989). A few longitudinal studies suggest causal relations between disc displacement and degenerative TMJ changes (Larheim, 2005; Kurita *et al.*, 2006); however, more evidence is needed to establish the consequences of disc displacement. Nevertheless, because TMJ eminence morphology provides important constraint forces in static mandibular biomechanics, and thus affects activities of muscles and subsequent TMJ loads during biting (Trainor *et al.*, 1995), TMJ disc displacement may have a bidirectional causal relationship with biomechanical differences in jaw systems. Therefore, the overall aim of this study was to investigate biomechanical differences in females and males with and without TMJ disc displacement. To date, no data have been presented to determine if effective eminence shapes in these four groups are significantly different, or if a numerical model based on joint load minimization can predict effective eminence shapes measured in individuals with disc displacement. This cross-sectional approach is a first step in elucidating causes for dynamic processes that result in disc displacement and which may lead to fatigue-failure of TMJ tissues. The working hypotheses tested in this project were that effective eminence shapes: (1) were not different for females and males with and without disc displacement, and (2) were consistent with joint load minimization in all groups of participants.

Materials & Methods

Participants

The study was approved by the Institutional Review Boards affiliated with the investigators. All participants gave informed consent. Inclusion criteria were: healthy dentitions without large restorations or large interdental spaces. Exclusion criteria were: arthritides, orofacial pain, gross asymmetries in clinically observable craniomandibular anatomy, and pregnancy as determined by medical histories and examination. Confirmation of clinical status was determined by a calibrated examiner using Research Diagnostic Criteria for TMDs (Dworkin and LeResche, 1992). Participants who met inclusion and exclusion criteria were categorized according to TMJ disc position as determined by a calibrated radiologist using magnetic resonance images (Ahmad *et al.*, 2009). Seventy-four individuals were recruited.

The same radiologist also confirmed the absence of osteo-arthritic structural changes using bilateral TMJ computed tomographs (Ahmad *et al.*, 2009). Thus, study samples were nine females and eight males of mean age 34 yrs (range, 20-57 yrs) with normally positioned TMJ discs bilaterally, and nine females and eight males of mean age 35 yrs (range, 19-62 yrs) with anteriorly displaced TMJ discs, bilaterally in 13 individuals and unilaterally in four individuals, with reduction in 21 joints and without reduction in 9 joints (Appendix Tables 1, 2). Power analyses on preliminary data indicated that \geq seven individuals *per* group would produce statistically significant results ($P < 0.04$).

Subject-specific Model-predicted and Measured Eminence Shapes

A geometry file was created for each participant with individual-specific anatomy in terms of three-dimensional coordinates describing relative positions of the: centered supero-antero-most point on each condyle; tooth row as represented by mandibular central incisors, canines, and first molars; and centroids of origins and insertions of 5 pairs of masticatory muscles (masseter, anterior temporalis, medial pterygoid, lateral pterygoid, anterior digastric). These data were determined from and checked for symmetry by standardized lateral and postero-anterior cephalometric radiographs of each participant according to previously described methods (Nickel *et al.*, 2003). We used each person's geometry file and a numerical modeling program to predict the unique effective sagittal TMJ eminence shape for that person. This modeling program used optimization based on minimization and equalization of left and right joint loads where direction of loading was unconstrained. The shape was generated and stored as a cubic polynomial and compared statistically with the bilateral effective sagittal TMJ eminence shapes measured by jaw-tracking in the same person in 2 repeated sessions separated by at least 1 day.

For the jaw-tracking, each participant performed a set of 10 protrusive-retrusive movements. A custom-made mandibular removable appliance and attached facebow delineated instantaneous positions of markers opposite the mandibular condyles through bilateral video recordings (Fig. 1). Ten right and left recordings were examined, and 2 or more smooth, complete, consecutive movements *per* side were selected and viewed frame-by-frame. Positions of each condylar marker relative to occlusal plane and 4 scaling coordinates were traced for consecutive frames, resulting in the *in vivo* effective sagittal eminence shape. Intra-operator reliability was assessed by tracings and measurements of 1 jaw-tracking session repeated on 10 different days. Maximum error in the method was ± 0.2 mm, or 3% of a maximum measured value of 5.9 mm.

Each tracing was quantified by means of a custom-made computer program that recorded at least 20 horizontal and vertical coordinates, corrected for scale, and calculated a best-fit cubic polynomial ($R^2 \geq 0.90$) that represented the experimentally measured effective eminence shape (Fig. 1). Four polynomials resulted for measured shapes from 2 sides and sessions for each participant and were compared in terms of steepness visually and *via* the first-order coefficients. We also used each polynomial to calculate the vertical dimensions of the measured effective eminence for a standardized horizontal series of 11 points 0.5 mm apart and parallel to occlusal plane, numbered 1-11 postero-anteriorly. The 11 points standardized condylar loading positions among subjects, where position #1 (0 mm, 0 mm in Figs. 2, 3) was defined as the point on the effective eminence opposite the centered supero-antero-most point on the condyle when the teeth were in maximum intercuspal position.

We used linear regression analysis to determine accuracy of model-predicted compared with measured data in each participant. Percent error was calculated as the difference between constants of proportionality for model-predicted *vs.* measured linear regression relations for each participant and a perfect-match (= 1.00).

Reliability, Left-Right Symmetry, and Statistical Analyses

We assessed inter-session reliability for measured effective eminence shapes on each side in the 34 participants by calculating intraclass correlation coefficients (ICCs). Based on this reliability analysis (see Results), measured eminence shapes from two sessions for a given side were averaged. Then, we assessed left-right symmetry in measured shapes for each participant using the sum of squared Euclidean distances of data from a perfectly symmetrical relationship with slope of 1.00 and intercept at the origin (Lele and Richtsmeier, 1991). That is, for each participant, values of eminence height (y) for the 11 horizontal points (x) were plotted left vs. right and compared with the line representing perfect symmetry. Finally, a repeated-measures analysis of covariance (ANCOVA) and Bonferroni-controlled tests compared vertical dimensions at given postero-anterior points (#2-11) for differences due to sex (female, male), group (without, with disc displacement), and method (predicted, measured).

Results

Differences in Measured Eminence Shapes

Measured effective sagittal eminence shapes exhibited significantly higher variability in steepness ($P = 0.01$) in those with (up to 10:1) compared with those without (up to 2:1) TMJ disc displacement (Figs. 2A, 2B).

Comparisons of Model-predicted and Measured Eminence Shapes

The numerical model accurately predicted the measured effective sagittal TMJ eminence shape of either left or right TMJ in most participants, where average absolute errors of 17% were found for best-matched and 36% for worst-matched sides (Appendix Tables 1, 2). Average absolute errors for the best-matched side were highest for females with disc displacement at 20% and lowest for males with disc displacement at 13%, whereas these were 15% for females and 18% for males without disc displacement.

We used linear regression analysis to compare vertical dimensions at horizontal points #2-11 for measured and predicted effective eminences in each participant (values for polynomials shown in Appendix Tables 1, 2). Average model-predicted and measured vertical dimensions of the effective eminence matched within a range of 0.0–0.6 mm for the 10 horizontal positions. These discrepancies increased postero-anteriorly.

Inter-session Reliability of Measured Eminence Shapes

Test-retest reliability between sessions was very good, with ICCs ranging from 0.86-0.98 on the left and 0.74-0.98 on the right. The lowest values were found at position #2 for both sides. The 95% confidence intervals were significantly different from zero ($P < 0.05$), indicating a high association between the measurements from two sessions. In addition, these intervals were widest at position #2 (left, 0.72-0.93; right, 0.49-0.87) and became narrower at each position up to position #9 (left, 0.96-0.99; right, 0.96-0.99). Thus, data from two sessions were averaged.

Left-Right Asymmetries in Measured Eminence Shapes

Five participants showed marked differences in left-right effective sagittal eminence shapes, where the average squared Euclidean distance was 25.92 mm² and ranged between 17.98 and 40.50 mm². These participants were considered to have left-right asymmetries. By comparison, squared Euclidean distances for the other 29 participants were low, where average squared Euclidean distance was 1.08 mm² and ranged between 0.05 and 6.34 mm². These participants were considered to have acceptable symmetry for comparison with

model-predicted results. Asymmetry, as defined above, occurred more often in participants with (24% of group; one female, three males) compared with those without TMJ disc displacement (6% of group; one male) (Figs. 3A-3E).

Comparison of Model-predicted and Measured Eminence Shapes for Symmetrical Subjects

Among 29 participants with acceptable left-right symmetry, neither group, nor sex, nor any other interactions showed significant effects. However, significant differences were found overall between model-predicted and measured vertical dimensions of the effective eminence for the 5 anterior-most points (#7-11; all $P < 0.01$, Table), which were toward the eminence crest.

Discussion

According to previous reports (Moffett *et al.*, 1964; Oberg *et al.*, 1971), the earliest and most frequent location of TMJ cartilage degeneration occurs at the eminence crest. The current results demonstrated that this is the area where effective sagittal eminence shape is least consistent with joint load minimization. However, overall, for up to 3.0 mm of condylar protrusion, there were no significant differences between predicted and measured effective eminence shapes. This suggests that, during loading of the mandible, when condyles are relatively posteriorly positioned, joint load minimization is optimized. This could apply for molar, canine, and incisor biting tasks in many individuals. For conditions where condylar protrusion of ≥ 3.0 mm is required to produce a biting force, effective eminence shapes are expected to be inconsistent with joint load minimization. Under these circumstances, the combination of joint load and stress concentration, due to surface incongruency (Nickel and McLachlan, 1994), may contribute to fatigue of the articulating fibrous connective tissues in some individuals.

Females with disc displacement showed generally more differences between predicted and measured shapes, which suggests that joint loads could be higher in this group and may partially explain the gender bias in TMDs. However, future studies are indicated with larger sample sizes and behavioral data characterizing frequency of loading and degree of condylar protrusion to elucidate more fully gender and diagnostic group differences in propensity to fatigue-failure of TMJ tissues.

Left-right asymmetry in measured effective eminence shapes occurred 4 times more often in participants with displaced TMJ discs compared with those with healthy TMJs. The current numerical modeling program assumes left-right symmetry, and the objective of joint load minimization quite successfully predicted measured effective eminence shape on at least one side, with an average error of 17%. In cases with measured left-right asymmetry, one side was inconsistent with predicted effective eminence shape based on joint load minimization. Given that the numerical model used joint load minimization to predict effective eminence shape, the results suggest that when there is asymmetry, joint loads are likely to be greater. Ideally, in future, left-right asymmetric anatomy and constraints of joint loads should be modeled to test these conditions more specifically. In addition, an improved definition of left-right eminence shape asymmetry should be established based on quantifiable biomechanical effects, derived from these improved models. Nevertheless, even the current modeling program identifies individuals who may and may not be prone to higher loading and, thus, to fatigue-failure of TMJ tissues, and suggests that joint conditions and behavior of these individuals should be followed longitudinally and compared.

In conclusion, a larger range of shapes (in terms of steepness) and higher prevalence of left-right shape asymmetries were measured in participants with anteriorly displaced TMJ discs compared with those with normally positioned discs. Furthermore, a numerical model based

on joint load minimization and the individual's anatomy successfully predicted effective sagittal eminence shape for up to 3.0 mm of condylar protrusion, but predicted and measured shapes beyond this were significantly different. Although speculative, if joint loads are not minimized when the condyle is more protruded, this may explain why tissue degeneration occurs earlier and more frequently at the eminence crest compared with other areas of the TMJ.

Supplementary Material

Refer to Web version on PubMed Central for supplementary material.

Acknowledgments

This work was supported by NIDCR R01DE16417 and is based, in part, on an MS thesis by M. Crosby, University of Nebraska Medical Center. The authors thank the participants, as well as Kim Theesen, graphic artist, and Theresa Speers, RN, BSN, research assistant.

References

- Ahmad M, Hollender L, Anderson Q, Kartha K, Ohrbach R, Truelove E, et al. Research diagnostic criteria for temporomandibular disorders (RDC/TMD): development of image analysis criteria and examiner reliability for image analysis. *Oral Surg Oral Med Oral Pathol Oral Radiol Endod.* 2009; 107:844–860. [PubMed: 19464658]
- Detamore MS, Athanasiou KA. Structure and function of the temporomandibular joint disc: implications for tissue engineering. *J Oral Maxillofac Surg.* 2003; 61:494–506. [PubMed: 12684970]
- Dworkin SF, LeResche L. Research diagnostic criteria for temporomandibular disorders: review, criteria, examinations and specifications, critique. *J Craniomandib Disord.* 1992; 6:301–355. [PubMed: 1298767]
- Gallo LM, Nickel JC, Iwasaki LR, Palla S. Stress-field translation in the healthy human temporomandibular joint. *J Dent Res.* 2000; 79:1740–1746. [PubMed: 11077988]
- Gallo LM, Chiaravalloti G, Iwasaki LR, Nickel JC, Palla S. Mechanical work during stress-field translation in the human TMJ. *J Dent Res.* 2006; 85:1006–1010. [PubMed: 17062740]
- Iwasaki LR, Baird BW, McCall WD Jr, Nickel JC. Muscle and temporomandibular joint forces associated with chincup loading predicted by numerical modeling. *Am J Orthod Dentofacial Orthop.* 2003a; 124:530–540. [PubMed: 14614421]
- Iwasaki LR, Petsche PE, McCall WD Jr, Marx D, Nickel JC. Neuromuscular objectives of the human masticatory apparatus during static biting. *Arch Oral Biol.* 2003b; 48:767–777. [PubMed: 14550379]
- Iwasaki LR, Thornton BR, McCall WD Jr, Nickel JC. Individual variations in numerically modeled human muscle and temporomandibular joint forces during static biting. *J Orofac Pain.* 2004; 18:235–245. [PubMed: 15509003]
- Kurita H, Uehara S, Yokochi M, Nakatsuka A, Kobayashi H, Kurashina K. A long-term follow-up study of radiographically evident degenerative changes in the temporomandibular joint with different conditions of disk displacement. *Int J Oral Maxillofac Surg.* 2006; 35:49–54. [PubMed: 15961278]
- Larheim TA. Role of magnetic resonance imaging in the clinical diagnosis of the temporomandibular joint. *Cells Tissues Organs.* 2005; 180:6–21. [PubMed: 16088129]
- Lawrence RC, Hochberg MC, Kelsey JL, McDuffie FC, Medsger TA Jr, Felts WR, et al. Estimates of the prevalence of selected arthritic and musculoskeletal diseases in the United States. *J Rheumatol.* 1989; 16:427–441. [PubMed: 2746583]
- Lele S, Richtsmeier JT. Euclidean distance matrix analysis: a coordinate-free approach for comparing biological shapes using landmark data. *Am J Phys Anthropol.* 1991; 86:415–427. [PubMed: 1746646]

- LeResche, L. Research diagnostic criteria for temporomandibular disorders. In: Friction, JR.; Dubner, R., editors. Orofacial pain and temporomandibular disorders. New York: Lippincott, Williams and Wilkins; 1995. p. 109-203.
- Moffett BC Jr, Johnson LC, McCabe JB, Askew HC. Articular remodeling in the adult human temporomandibular joint. *Am J Anat.* 1964; 115:119–141. [PubMed: 14199779]
- National Institute of Dental and Craniofacial Research Web site. [accessed Feb 3, 2010] Facial pain; prevalence of TMJD and its signs and symptoms.
<http://www.nidcr.nih.gov/DataStatistics/FindDataByTopic/FacialPain/>
- Nickel, JC.; Iwasaki, LR. In vivo tests of TMJ morphology and masticatory muscle forces predicted by computer-assisted models. In: Davidovitch, Z.; Mah, J., editors. Biological mechanisms of tooth movement and craniofacial adaptation. Boston: Harvard Society for the Advancement of Orthodontics; 2004. p. 63-74.
- Nickel JC, McLachlan KR. An analysis of surface congruity in the growing human temporomandibular joint. *Arch Oral Biol.* 1994; 39:315–321. [PubMed: 8024496]
- Nickel JC, McLachlan KR, Smith DM. Eminence development of the postnatal human temporomandibular joint. *J Dent Res.* 1988; 67:896–902. [PubMed: 3170901]
- Nickel JC, Iwasaki LR, Feely DE, Stormberg KD, Beatty MW. The effect of disc thickness and trauma on disc surface friction in the porcine temporomandibular joint. *Arch Oral Biol.* 2001; 46:155–162. [PubMed: 11163323]
- Nickel JC, Yao P, Spalding PM, Iwasaki LR. Validated numerical modeling of the effects of combined orthodontic and orthognathic surgical treatment on TMJ loads and muscle forces. *Am J Orthod Dentofacial Orthop.* 2002; 121:73–83. [PubMed: 11786875]
- Nickel JC, Iwasaki LR, Walker RD, McLachlan KR, McCall WD Jr. Human masticatory muscle forces during static biting. *J Dent Res.* 2003; 82:212–217. [PubMed: 12598551]
- Oberg T, Carlsson GE, Fajers CM. The temporomandibular joint. A morphologic study on a human autopsy material. *Acta Odontol Scand.* 1971; 29:349–384. [PubMed: 5286674]
- Trainor PG, McLachlan KR, McCall WD. Modelling of forces in the human masticatory system with optimization of the angulations of the joint loads. *J Biomech.* 1995; 28:829–843. [PubMed: 7657681]

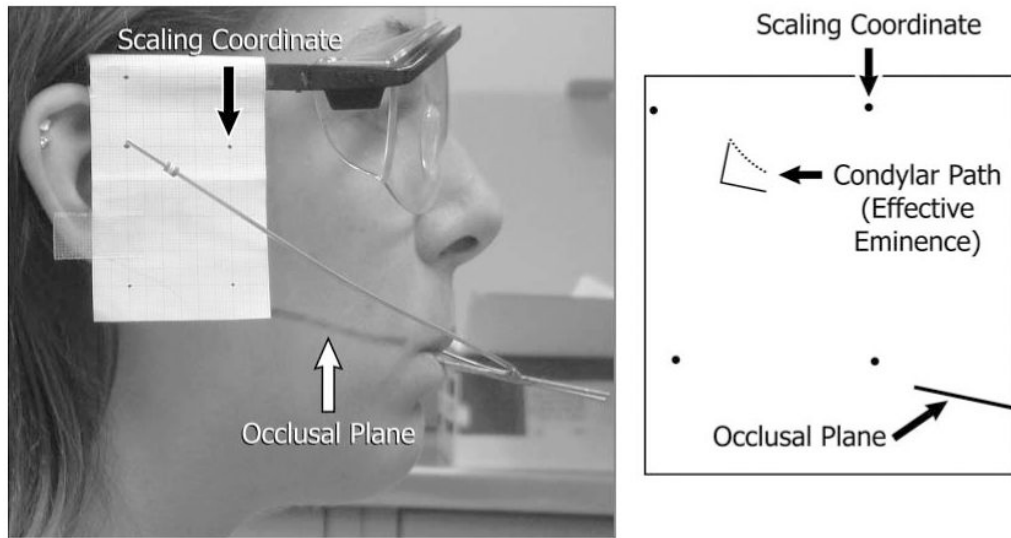


Figure 1.

Image of a participant (left) during jaw-tracking and tracing of path of condylar marker (right) relative to occlusal plane. Scaling coordinates are shown as recorded and reproduced in the tracing. Perpendicular lines represent the axis system used in Figs. 2 and 3.

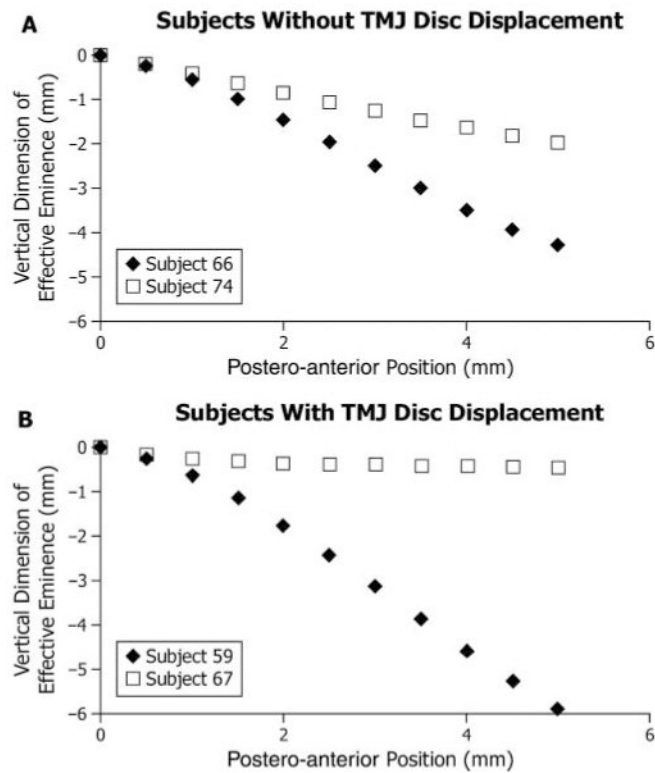


Figure 2.

Extremes of effective sagittal TMJ eminence shape among (A) participants without TMJ disc displacement ($n = 17$) and (B) those with TMJ disc displacement ($n = 17$), where vertical dimension of the eminence (mm) is plotted on the vertical axis vs. postero-anterior position (mm, positions #1-11) on the horizontal axis. The horizontal axis is parallel to the occlusal plane. Position #1 (0 mm, 0 mm) was defined as the point on the effective eminence opposite the centered supero-antermost point on the condyle when the teeth were in maximum intercuspal position. For each diagnostic group, the participant with the steepest eminence was identified by ◆, while the participant with the flattest eminence was identified by □.

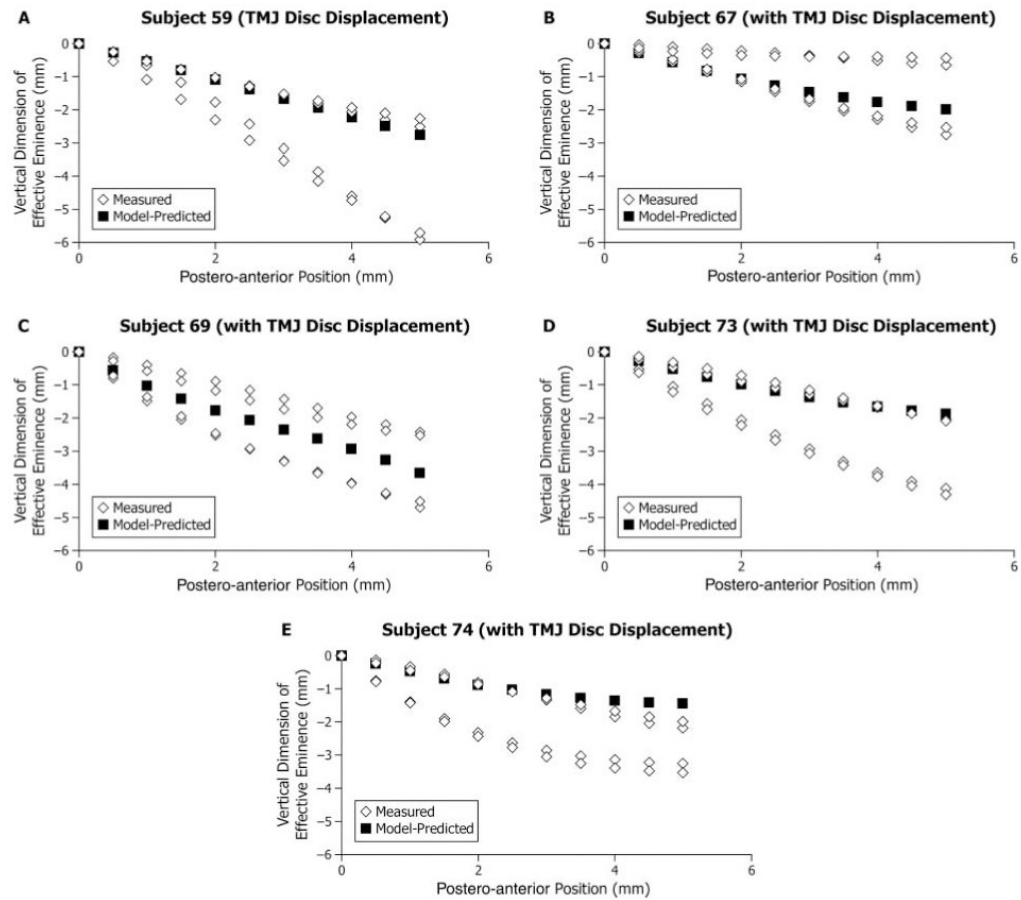


Figure 3.

Participants with left-right asymmetry in effective sagittal TMJ eminence shape: (**A-D**) Four participants with TMJ disc displacement and (**E**) one participant without TMJ disc displacement. Model-predicted shape (■) and measured shapes (◇) for the right and left sides and two experimental sessions are plotted showing vertical dimension of effective eminence (mm) on the vertical axis and postero-anterior position (mm, positions #1-11) on the horizontal axis. The horizontal axis is parallel to the occlusal plane. Position #1 (0 mm, 0 mm) was defined as the point on the effective eminence opposite the centered supero-anteromost point on the condyle when the teeth were in maximum intercuspal position.

Table
Results of Analysis of Covariance and Bonferroni *post hoc* Tests for Effects of Method (model-predicted, measured) and Postero-anterior Position on Vertical Dimension of the Effective Sagittal TMJ Eminence with Sex and Diagnostic Group as Fixed Factors (with estimated least-square means and degrees of freedom = 525, where standard error = 0.1)

Position #	Postero-anterior Distance (mm)	Vertical Dimension (mm)		Bonferroni-adjusted P
		Model-predicted	Measured	
1	0.0	0.0	0.0	10.00
2	0.5	-0.4	-0.4	7.32
3	1.0	-0.8	-0.9	4.30
4	1.5	-1.2	-1.3	1.84
5	2.0	-1.5	-1.6	0.54
6	2.5	-1.8	-2.0	0.09
7	3.0	-2.0	-2.3	0.01
8	3.5	-2.3	-2.6	0.01
9	4.0	-2.5	-2.9	< 0.01
10	4.5	-2.7	-3.2	< 0.01
11	5.0	-2.8	-3.4	< 0.01